J. Cent. South Univ. Technol. (2010) 17: 1095−1102
DOI: 10.1007/s11771−010−0602−5

Springer

Strength and deformation behaviour of coarse-grained soil by true triaxial tests

SHI Wei-cheng(施维成)[1, 2], ZHU Jun-gao(朱俊高)[1], CHIU Chung-fai(赵仲辉)[1], LIU Han-long(刘汉龙)[1]

1. Key Laboratory of Ministry of Education for Geomechanics and Embankment Engineering, Hohai University, Nanjing 210098, China;
2. School of Civil Engineering and Architecture, Changzhou Institute of Technology, Changzhou 213002, China

Abstract: In order to investigate the influence of intermediate principal stress on the stress−strain and strength behaviour of a coarse-grained soil, a series of true triaxial tests were performed. The tests were conducted in a recently developed true triaxial apparatus with constant minor principal stress σ_3 and constant value of intermediate principal stress ratio $b=(\sigma_2-\sigma_3)/(\sigma_1-\sigma_3)$ (σ_1 is the vertical stress, and σ_2 is the horizontal stress). It is found that the intermediate principal strain, ε_2, increases from negative to positive value with the increase of parameter b from zero to unity under a constant minor principal stress. The minor principal strain, ε_3, is always negative. This implies that the specimen exhibits an evident anisotropy. The relationship between b and friction angle obtained from the tests is different from that predicted by LADE-DUNCAN and MATSUOKA-NAKAI criteria. Based on the test results, an empirical equation of $g(b)$ that is the shape function of the failure surface on π-plane was presented. The proposed equation is verified to be reasonable by comparing the predicted results using the equation with true triaxial test results of soils, such as coarse-grained soils in this study, sands and gravels in other studies.

Key words: cohesionless soil; coarse-grained soil; true triaxial test; strength; deformation; failure criterion

1 Introduction

Conventional triaxial tests are widely used to investigate the deformation and strength behavior of various soils including clays, sands and coarse-grained soils [1]. The stress paths for these tests, however, are often limited to axial-symmetric stress state that may not be similar to those encountered in the field. In fact, the behavior of soil under general three-dimensional stress states is quite different from that of soil in axial-symmetric stress state [2−3], and thus a number of true triaxial apparatuses were developed [4−7]. On the other hand, torsional shear test is the alternative for the study of behaviour of soil under general three-dimensional stress states [8−10]. LADE et al [8] performed 34 drained torsion shear tests on hollow cylinder specimens of Santa Monica Beach sand to investigate the behavior of the sand. LIN et al [9] found that the yielding behavior and failure criteria were strongly dependent on the principal stress rotation angle (β) and plastic work through combined axial-torsional tests on hollow cylindrical specimens of kaolin clay. LADE and KIRKGARD [10] investigated the influence of stress rotation and changes in b-values on the stress−strain, pore pressure, and strength behaviour of the clays through a series of consolidated-undrained torsion shear tests on hollow cylindrical specimens of undisturbed San Francisco Bay mud. For coarse-grained soils, however, it is difficult to prepare hollow cylinder specimens, so the true triaxial apparatus was chosen in this study.

True triaxial apparatuses were classified into three categories according to the type of boundary conditions [11]: (Ⅰ) all six faces of a cubical specimen are loaded by flexible bags; (Ⅱ) the vertical stress is applied through a rigid boundary, one horizontal stress is applied by the cell pressure, and the other is applied by the cell pressure and an additional deviator stress; and (Ⅲ) all six faces are loaded by rigid platens.

So far many true triaxial tests were performed on clays or sands [12−14]. LADE and DUNCAN [12]

Foundation item: Project(50639050) supported by the National Natural Science Foundation of China and Er-Tan Hydraulicpower Limited Company; Project (50579014) supported by the National Natural Science Foundation of China; Project(09KJD560003) supported by the Natural Science Foundation of Jiangsu Higher Education Institutions of China; Project(BK2007582) supported by Jiangsu Provincial Natural Science Foundation of China; Project(20070294002) supported by the Specialized Research Fund for the Doctoral Program of Higher Education of China; Project(GH200904) supported by Key Laboratory of Ministry of Education for Geomechanics and Embankment Engineering, Hohai University, China
Received date: 2009−11−18; **Accepted date**: 2010−03−16
Corresponding author: ZHU Jun-gao, PhD, Professor; Tel: +86−25−83787217; E-mail: zhujungao@hhu.edu.cn

designed a cubical triaxial apparatus which was type Ⅱ in the above classifications and performed a series of tests including plane strain tests and tests with constant value of b. ABELEV and LADE [13] conducted an extensive experimental investigation on Santa Monica beach sand, and these true triaxial tests covered the entire range of values of Lode angle, from 0 to 180°. JAFARZADEH et al [14] performed a series of true triaxial tests in different stress paths with at p=200 kPa.

Based on the true triaxial test results, some failure criteria were proposed like LADE and DUNCAN [4] and MATSUOKA and NAKAI [15]. Recently, some more advanced criteria have been presented to capture the behavior of sand and clay [16]. At the same time, some numerical tests were performed to study the strength behaviors [17−18].

Although a lot of experimental studies were performed to investigate three-dimensional behavior of clays and sands, few of them were on coarse-grained soil.

Coarse-grained soils were widely used in the construction of earth rockfill dams [19]. VARADARAJAN et al [20] conducted drained triaxial tests on modeled rockfill materials and developed a constitutive model to predict their stress−stain−volume change behavior. Although a large number of experimental studies were carried out on these soils to investigate their mechanical properties, most of them were conducted in conventional triaxial test. No results of coarse-grained soils could be found from true triaxial test.

In the present study, the deformation and strength of a coarse-grained soil by using true triaxial tests were investigated. The effect of a stress parameter b (b=(σ_2−σ_3)/(σ_1−σ_3), σ_1 is the vertical stress, and σ_2 is the horizontal stress) on the deformation and strength was analyzed.

2 True triaxial tests

2.1 True triaxial apparatus

In the true triaxial test, vertical load was applied through a rigid plate, and one horizontal load was passed to specimen by a specially designed block similar to that used by LADE and DUNCAN [12]. The other horizontal load was applied by a flexible water bag [21]. The size of the cubical specimen was 12 cm× 12 cm×6 cm.

2.2 Soil tested

The coarse-grained soil used was obtained from Shuangjiangkou earth rockfill dam on Daduhe River, China. The grain size distribution of the tested soil is listed in Table 1.

Table 1 Grain size distribution of tested soil

Grain size/mm	10	5	2	1	0.5	0.075
Percentage finer/%	100.0	30.0	21.5	18.8	12.9	3.0

The maximum and minimum densities of the soil were 1.96 and 1.54 g/cm^3, respectively, and the particle of the coarse grain was a type of gray granite whose maximum grain size was 10 mm. The uniformity coefficient of the specimen was 24, and the coefficient of curvature was 12.

2.3 Testing program

All the specimens were prepared by compaction to the same density. The density of specimen tested was 1.91 g/cm^3, and the relative density (D_r) was 90.4%. All the tests were conducted on dry specimens.

All the true triaxial tests were performed with constant minor principal stress σ_3 and constant value of b. During the test horizontal stress σ_2 and vertical stress σ_1 are increased proportionally to keep constant b until the specimen reaches failure. The values of b were chosen as 0, 0.25, 0.50, 0.75, 1.00, and the minor principal stresses were 200, 300, 400 kPa.

3 Strength and stress−strain behavior

3.1 Stress−strain relationship

Fig.1 presents the relationship between σ_1−σ_3 and major principal strain ε_1 for the coarse-grained soil at different values of b and σ_3. It can be seen that the strength is the lowest for the conventional triaxial compression (b=0) under a given σ_3. In general, the strength increases with the increase of σ_3 for a given value of b except that the strength decreases with increasing value of b from 0.75 to 1.00 at σ_3=200 kPa, as shown in Fig.1(a).

3.2 Relationships between principal stains

The relationship curves between intermediate principal strain ε_2 and major principal strain ε_1 are plotted in Fig.2. The figure shows that the intermediate principal strains are negative when b is equal to zero and positive when b varies from 0.25 to unity. Here, negative strain means expansion. With the increase of parameter b, ε_2 increases considerably.

Fig.3 shows the relationship between ε_3 and ε_1, which indicates that the minor principal strains are expansive in all cases of tests and decrease with increasing b for a given minor principal stress. On the

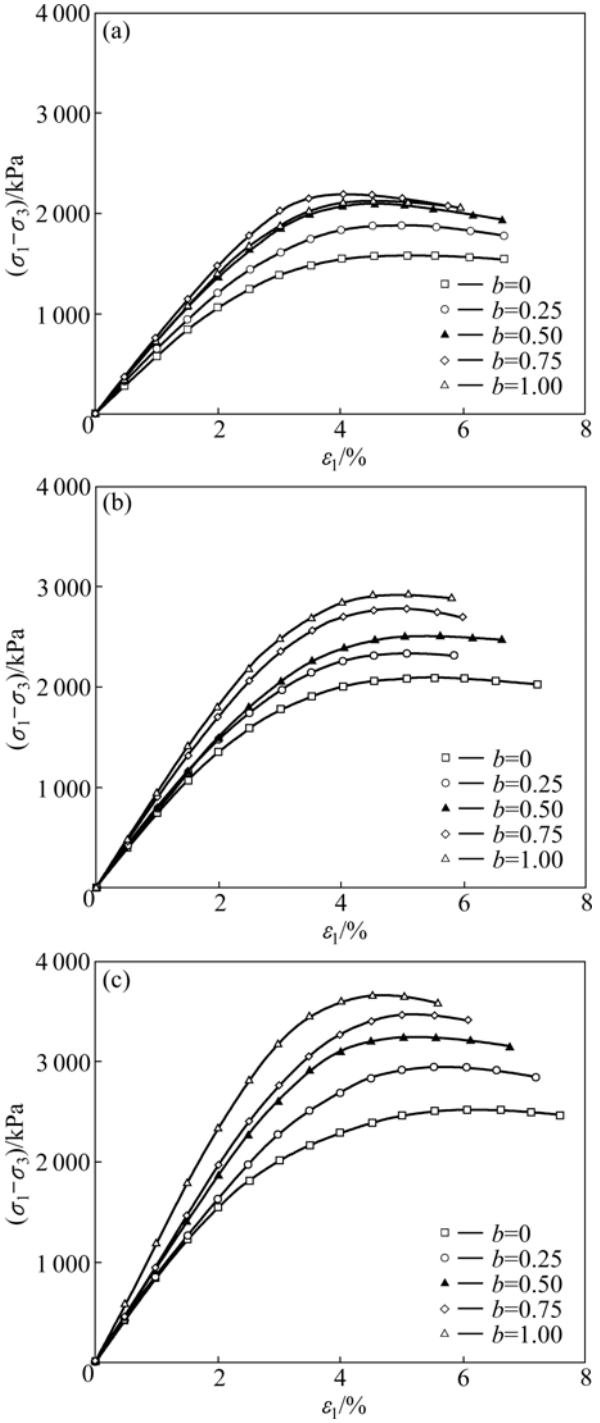

Fig.1 Relationship between $\sigma_1-\sigma_3$ and ε_1 at different σ_3 values: (a) σ_3=200 kPa; (b) σ_3=300 kPa; (c) σ_3=400 kPa

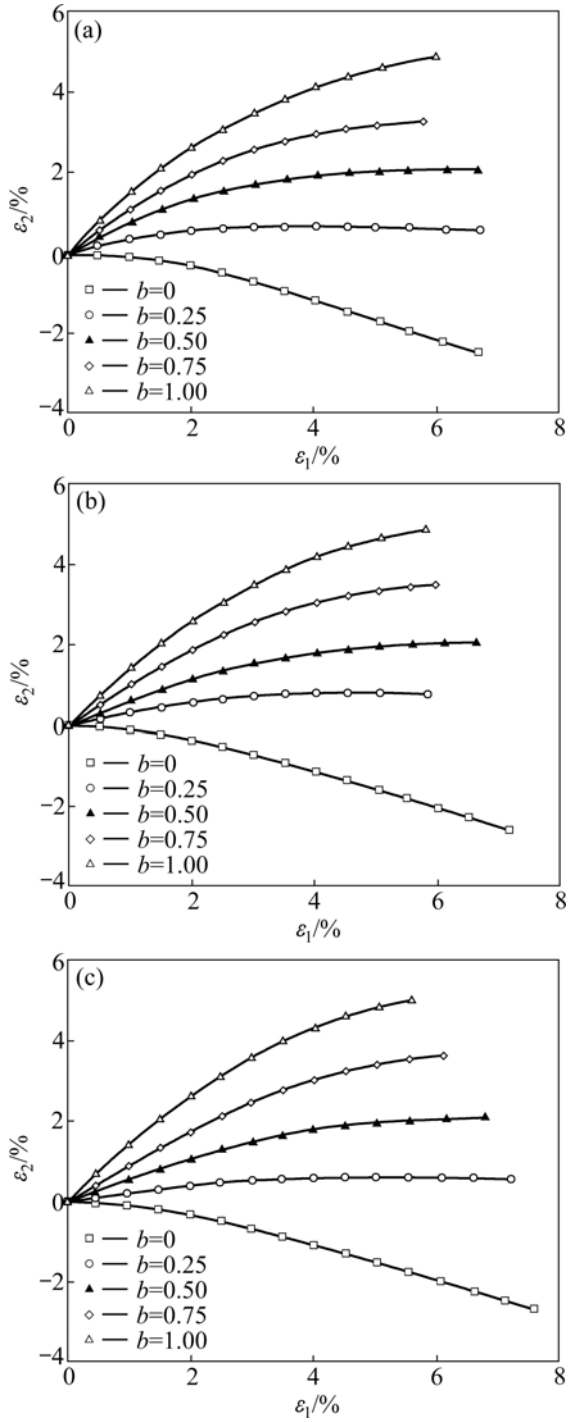

Fig.2 Relationship between ε_2 and ε_1 at different σ_3 values: (a) σ_3=200 kPa; (b) σ_3=300 kPa; (c) σ_3=400 kPa

other hand, with the increase of minor principal stress, ε_3 increases for a given b.

3.3 Peak friction angle

Peak friction angle (φ) is commonly used to evaluate the peak strength. It is well known that the friction is related to σ_2, the $\varphi-b$ diagram is widely used to represent the variation of φ under three-dimensional stress conditions, and φ is calculated for cohesionless soil by

$$\varphi = \arcsin\frac{\sigma_{1f}-\sigma_{3f}}{\sigma_{1f}+\sigma_{3f}} \tag{1}$$

where σ_{1f} and σ_{3f} are major principal stress and minor principal stress at failure, respectively.

Fig.4 illustrates the variation of φ with b at a constant minor principal stress. The predictions from the failure criteria proposed by LADE and DUNCAN [4] and

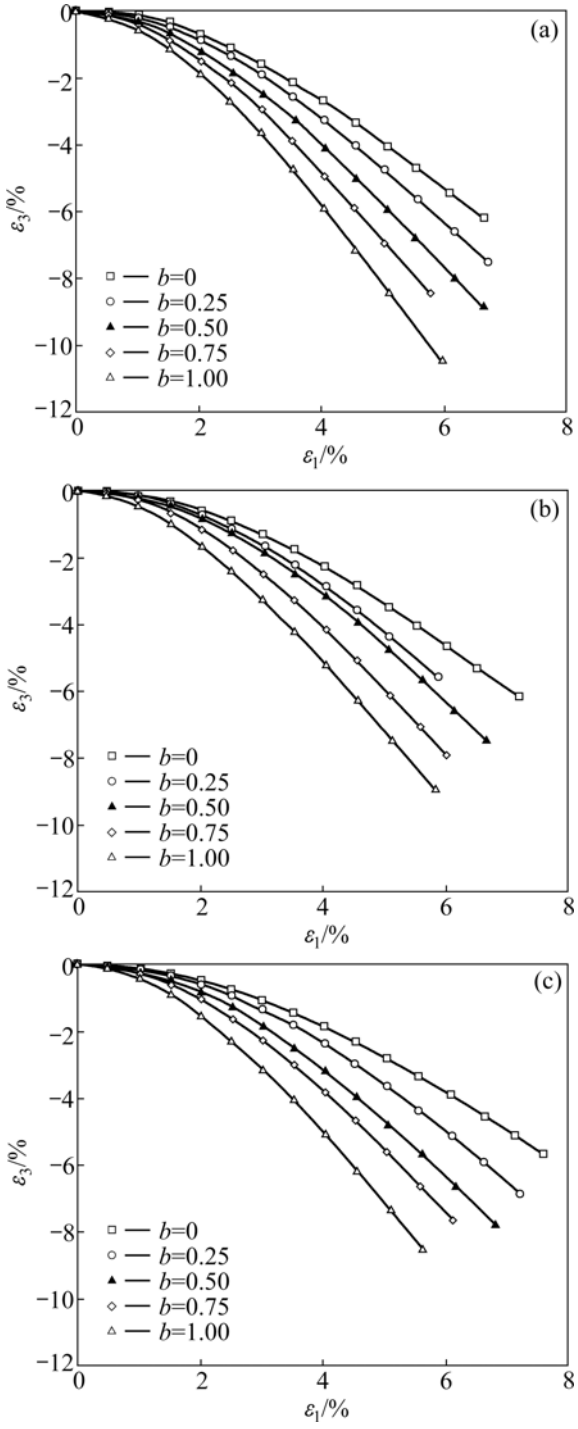

Fig.3 Relationship between ε_3 and ε_1 at different σ_3 values: (a) σ_3=200 kPa; (b) σ_3=300 kPa; (c) σ_3=400 kPa

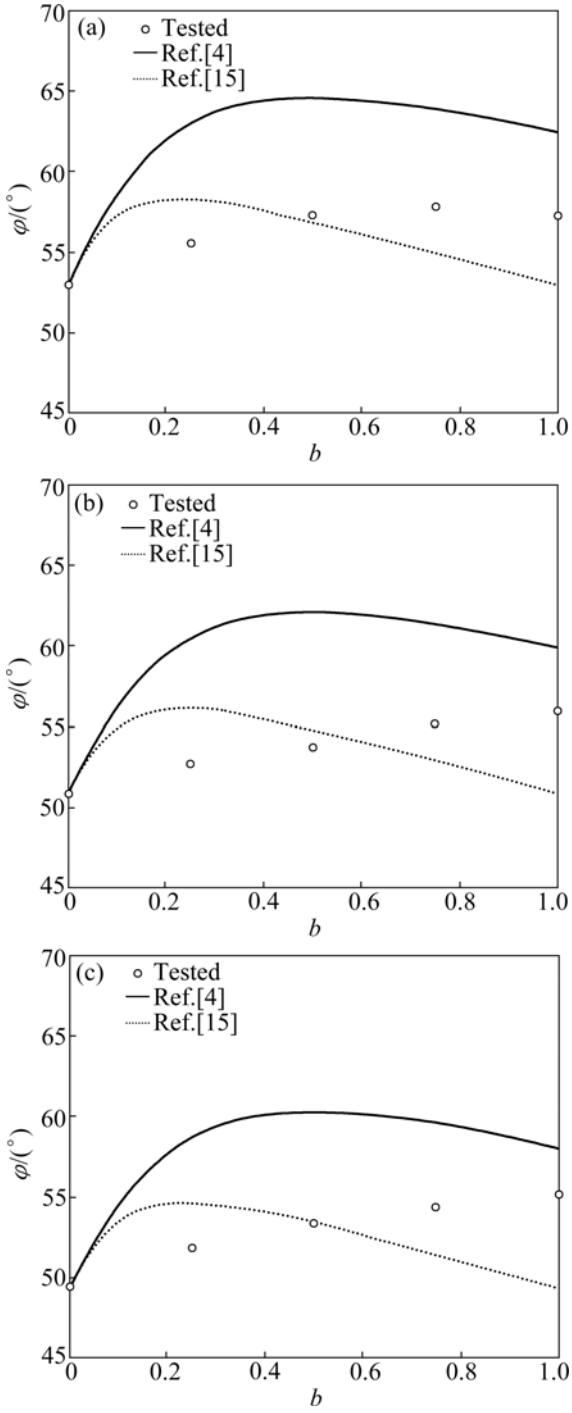

Fig.4 Variations of friction angle (φ) with parameter (b) at different σ_3 values: (a) σ_3=200 kPa; (b) σ_3=300 kPa; (c) σ_3=400 kPa

MATSUOKA and NAKAI [15] are also shown in the figure for comparison.

It can be seen from Fig.4 that the measured friction angle from the conventional triaxial compression (b=0) is the smallest in all the tests. In general, the friction angle increases with increasing value of b, except that it decreases with increasing value of b from 0.75 to 1.00 for σ_3=200 kPa, as shown in Fig.4(a).

The tested results shown in Fig.4 do not agree well with the predictions of the two failure criteria. The friction angle predicted from MATSUOKA-NAKAI criterion [15] for conventional triaxial extension (b=1) is equal to that for conventional triaxial compression (b=0), while the friction angle measured in the conventional triaxial extension is larger than that measured in the conventional triaxial compression. This phenomenon can be depicted by LADE-DUNCAN failure criterion [4], but the predictions from this criterion as shown in Fig.4

overrate the influence of b value on the friction angle.

3.4 Shape function of failure surface on π-plane

The measured peak stress ratio (M) is defined as

$$M=\frac{q_{\mathrm{f}}}{p_{\mathrm{f}}} \tag{2}$$

where p_{f} and q_{f} are the mean stress and generalized deviator stress at failure.

The variation of M with b at different σ_3 values is shown in Fig.5. It can be seen from Fig.5 that the measured peak stress ratio decreases with increasing b for a given minor principal stress and decreases with increasing minor principal stress for a given b. The measured peak stress ratio M decreases substantially at a smaller b, and the decrement with respect to b reduces significantly at a larger b.

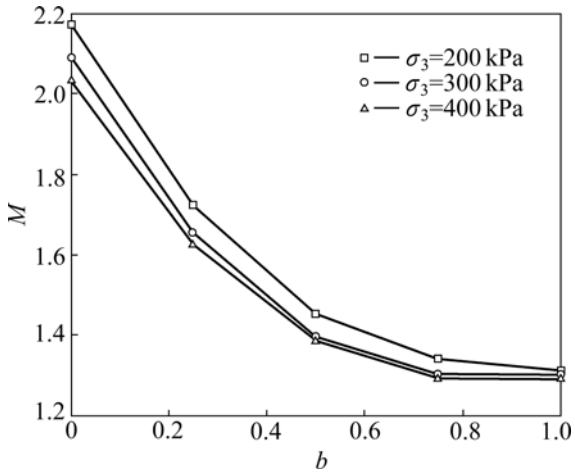

Fig.5 Variation of peak stress ratio (M) at failure with b at different σ_3 values

It was found by many investigators that the friction angle of cohesionless soil (φ_{c}) in the conventional triaxial stress condition decreases with increasing the magnitude of minor principal stress (σ_3), which could be expressed as [22]

$$\varphi_{\mathrm{c}}=\varphi_0-\Delta\varphi\cdot\lg\left(\frac{\sigma_3}{p_{\mathrm{a}}}\right) \tag{3}$$

where p_{a} is the atmospheric pressure; φ_0 is the friction angle for $\sigma_3=p_{\mathrm{a}}$; and $\Delta\varphi$ reflects the degree of the decrease of the friction angle with σ_3. For the soil tested in this work, φ_0=55.6° and $\Delta\varphi$=9.2°.

In many constitutive models, for example, Cam-clay model, constant M is assumed. This implies that on π-plane the failure track is a circle. Even if Eq.(3) is used, the influence of σ_2 on the strength can still not be taken into account. In fact, for an arbitrary three-dimensional stress state in which $b\neq0$, the influence of σ_2 on the strength is evident. It is significant to establish the relationship between the strength and the value of b or Lode angle (θ_σ). A number of researchers have studied on this problem for years. An effective way is to use a shape function on π-plane. The shape function, $g(\theta_\sigma)$, which is a function of θ_σ, is often used [23]. Function $g(\theta_\sigma)$ determines the shape of failure surface on π-plane.

It is of interest to introduce a shape function, $g(b)$, which is similar to $g(\theta_\sigma)$ and defined as

$$g(b)=\frac{q_{\mathrm{f}}}{q_{\mathrm{cf}}} \tag{4}$$

where q_{cf} is the deviator stress in the conventional triaxial compression (b=0). On π-plane there is the same value of mean stress, thus $g(b)$ can be given by using Eq.(2)

$$g(b)=\frac{M}{M_{\mathrm{c}}} \tag{5}$$

where M_{c} is the peak stress ratio in the conventional triaxial compression (b=0).

Fig.6 shows the relationship between $g(b)$ and b for the tested coarse-grained soil. It is found that the measured data in Fig.6 can be fitted by

$$g(b)=\frac{1}{(1+k)-k(b-1)^2} \tag{6}$$

where k is the parameter varying with minor principal stress σ_3, as shown in Fig.6 and listed in Table 2. It can be seen from Fig.6 that for different minor principal stresses, the simulated lines fit well with the test data. Eq.(6) is quite simple and can be used. In Eq.(6), $g(0)$=1 at b=0, and $g(1)$=1/(1+k) at b=1. This implies that at b=1 the strength from Eq.(6) is greater than that from MOHR-COULOMB criterion.

In order to verify Eq.(6), the relationships between $g(b)$ and b obtained from the true triaxial tests for loose sand and dense sands performed by LADE and DUNCAN [12] and for fine gravel performed by SHI et al [24] were simulated by Eq.(6), as shown in Fig.7. For loose sand, k=0.40 in Fig.7(a), k=0.46 in Fig.7(b) for dense sand, and k=0.56 in Fig.7(c) for fine gravel (Table 2). It can be seen that the simulated results by Eq.(6) are in good agreement with the tested results for loose sand, dense sand and fine gravel.

It is well known that so far most of the shape functions of failure surface on π-plane are only related to θ_σ and friction angle from conventional triaxial compression test. From Eq.(6) and Fig.6, however, it seems that $g(b)$ is related to b and σ_3 as b is equivalent to θ_σ. For the coarse-grained soil tested, the friction angle changes with minor principal stress σ_3 due to particle crashing. Therefore, it is assumed that parameter k is

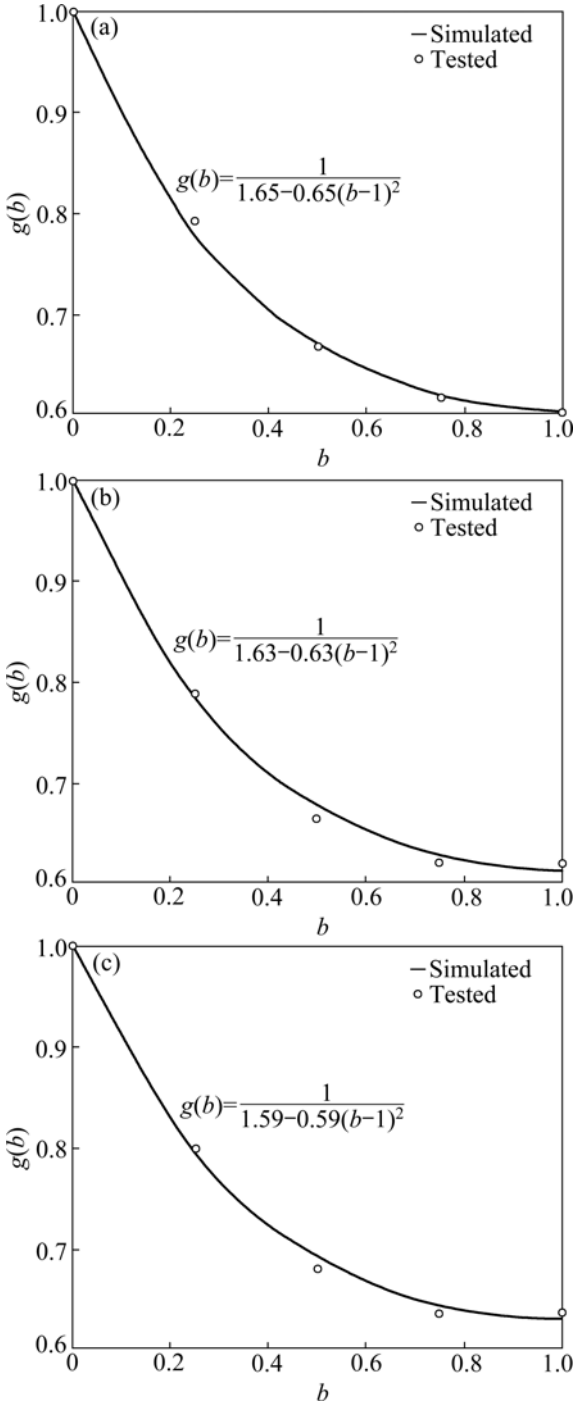

Fig.6 Simulation of shape function $g(b)$ for coarse-grained soil at different σ_3 values: (a) σ_3=200 kPa; (b) σ_3=300 kPa; (c) σ_3=400 kPa

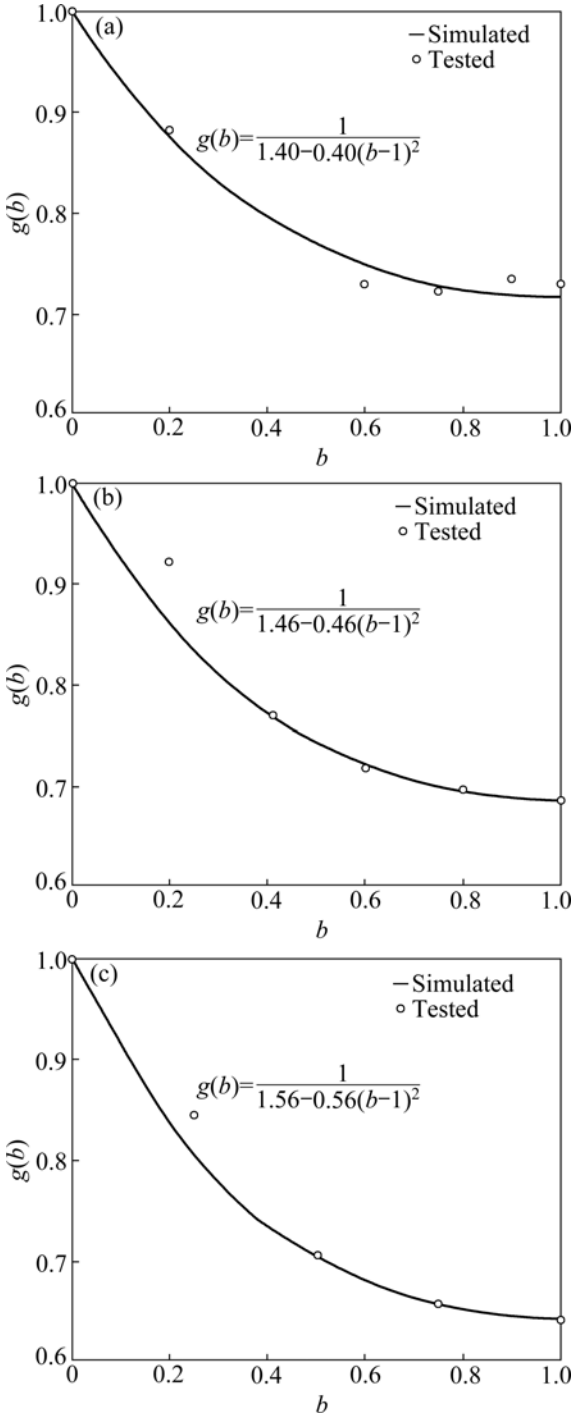

Fig.7 Verification of shape function $g(b)$ at different σ_3 values: (a) σ_3=49 kPa, loose sand; (b) σ_3=100 kPa, dense sand; (c) σ_3=400 kPa, fine gravel

Table 2 Friction angle and parameter k of different samples

Source	Case	φ_c/(°)	k
This work	σ_3=200 kPa	52.8	0.65
	σ_3=300 kPa	51.2	0.63
	σ_3=400 kPa	50.1	0.59
Ref.[12]	Loose sand	38.6	0.40
	Dense sand	42.8	0.46
Ref.[24]	Fine gravel	48.6	0.56

related to the friction angle. As a result, $g(b)$ is assumed to relate to b and φ_c. Using Eq.(3) and φ_0=55.6°, $\Delta\varphi$=9.2°, φ_c can be found for the tested soil at σ_3=200, 300 and 400 kPa, as listed in Table 2.

For loose and dense sands, the friction angles are respectively 38.6° and 42.8° [12], and 48.6° for fine gravel [24], which are also listed in Table 2.

The relationship between k and φ_c is plotted on k−

$\sin\varphi_c$ plane using data in Table 2, as shown in Fig.8. It is found that the relationship between k and $\sin\varphi_c$ is linear and can be fitted by

$$k = 1.462\sin\varphi_c - 0.523\,2 \tag{7}$$

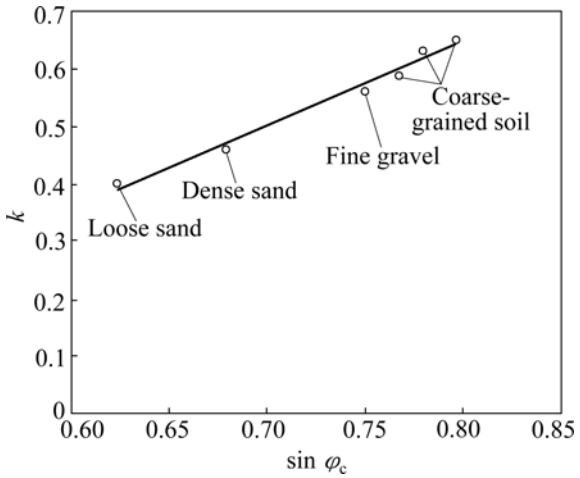

Fig.8 Relationship between k and $\sin\varphi_c$

By combining Eq.(5) with Eq.(6) a failure criterion may be found

$$q = \frac{pM_c}{(1+k)-k(b-1)^2} \tag{8}$$

If this equation is satisfied, the element is then in a state of failure.

3.5 Discussion on shape function

Eq.(6) actually defines a failure criterion for cohesionless soil, and thus it is valuable to further investigate the shape of failure surface on π-plane.

From Eq.(6) it is found that when b=1, $\partial g(b)/\partial b$=0, and when b=0, $\partial g(b)/\partial b$=−2k≠0. This implies that at b=1 the shape function is continuous, and at b=0 it is not continuous.

Eq.(6) can reflect the effect of σ_2. The shapes of failure criteria on π-plane are shown in Fig.9. For convenient comparison, the shapes of LADE-DUNCAN, MATSUOKA-NAKAI and MOHR-COULOMB criteria are also presented in Fig.9(a). It shows that the current criterion is located between LADE-DUNCAN and MOHR-COULOMB criteria.

Fig.9(b) illustrates the shapes of the presented criterion at φ_c=15°, 25°, 35° and 45°. It shows that the difference between g(0) and g(1) increases with the increase of friction angle.

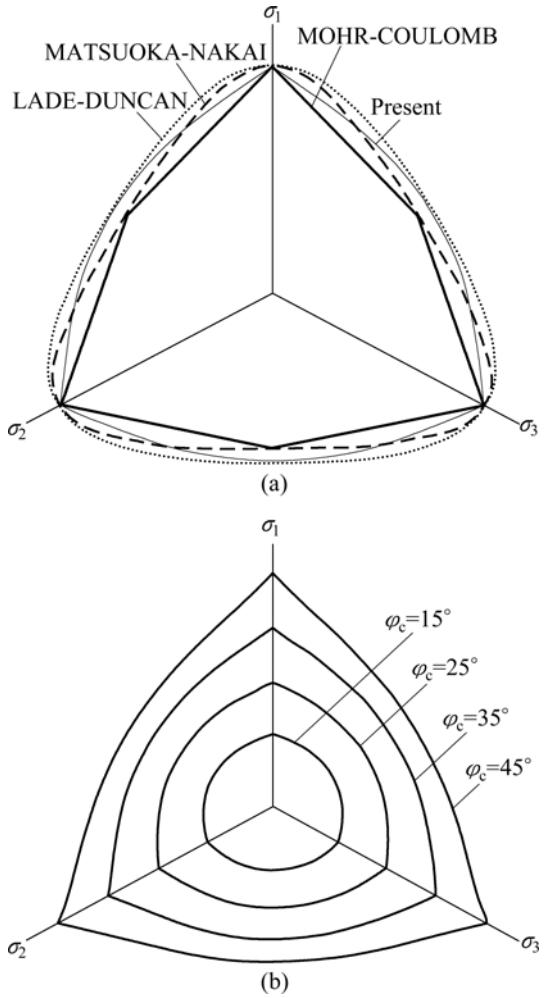

Fig.9 Shapes of failure criteria on π-plane: (a) Shapes of different criteria; (b) Shapes of presented criterion at different φ_c values

4 Conclusions

(1) A number of true triaxial tests are performed. The test results show that the strength is lowest in the conventional triaxial compression condition (b=0) compared with that in other conditions (b≠0). The intermediate principal strain increases from negative to positive with increasing b from zero to unity. The minor principal strain is negative for all the b values, which decreases with the increase of b.

(2) Comparing φ−b relationship measured in the true triaxial tests and those depicted by LADE-DUNCAN and MATSUOKA-NAKAI failure criteria, it can be found that the test results do not agree well with the predicted results of the two failure criteria.

(3) A shape function, $g(b)$, of failure surface on π-plane is presented. The validity of the function is confirmed by using true triaxial test results of coarse-grained soil, sand, and fine gravel in other studies. The proposed shape function and the failure criterion can reasonably reflect the strength of cohesionless soil. More studies, including performing true triaxial tests at higher pressures, are necessary to verify the failure criterion.

References

[1] HAERI S M, HOSSEINI S M, TOLL D G, YASREBI S S. The behaviour of an artificially cemented sandy gravel [J]. Geotechnical and Geological Engineering, 2005, 23: 537−560.

[2] ZHU H N, MEHRABADI M M, MASSOUDI M. Three-dimensional constitutive relations for granular materials based on the dilatant double shearing mechanism and the concept of fabric [J]. International Journal of Plasticity, 2006, 22: 826−857.

[3] GEORGIADIS K, POTTS D M, ZDRAVKOVIC L. Modelling the shear strength of soils in the general stress space [J]. Computers and Geotechnics, 2004, 31: 357−364.

[4] LADE P V, DUNCAN J M. Elastoplastic stress−strain theory for cohesionless soil [J]. Journal of the Geotechnical Engineering Division, 1975, 101(10): 1037−1053.

[5] DOUQLAS M, DAYAKAR P. True triaxial testing system for clay with proportional-integral-differential (PID) control [J]. Geotechnical Testing Journal, 2004, 27(2): 134−144.

[6] KHALID A A, HEATH S W. A true triaxial apparatus for soil testing with mixed boundary conditions [J]. Geotechnical Testing Journal, 2005, 28(6): 534−543.

[7] CHOI C H, PEDRO A, MICHAEL D H. Development of a true triaxial apparatus for sands and gravels [J]. Geotechnical Testing Journal, 2008, 31(1): 32−44.

[8] LADE P V, MAM J, HONG W P. Interpretation of strains in torsion shear tests [J]. Computers and Geotechnics, 2009, 36: 211−225.

[9] LIN H, PRASHANT A, PENUMADU D. Single hardening elasto-plastic model for kaolin clay with loading-history-dependent plastic potential function [J]. International Journal of Geomechanics, 2006, 6(1): 55−63.

[10] LADE P V, KIRKGARD M M. Effects of stress rotation and changes of *b*-values on cross-anisotropic behavior of natural K_0-consolidated soft clay [J]. Soils and Foundations, 2000, 40(6): 93−105.

[11] LADE P V. Assessment of test data for selection of 3-D failure criterion for sand [J]. International Journal for Numerical and Analytical Methods in Geomechanics, 2006, 30: 307−333.

[12] LADE P V, DUNCAN J M. Cubical triaxial tests on cohesionless soil [J]. Journal of the Soil Mechanics and Foundations Division, 1973, 99(10): 793−812.

[13] ABELEV A V, LADE P V. Effects of cross anisotropy on three-dimensional behavior of sand (I): Stress−strain behavior and shear banding [J]. Journal of Engineering Mechanics, 2003, 129(2): 160−166.

[14] JAFARZADEH F, JAVAHERI H, SADEK T, MUIR WOOD D. Simulation of anisotropic deviatoric response of hostun sand in true triaxial tests [J]. Computers and Geotechnics, 2008, 35: 703−718.

[15] MATSUOKA H, NAKAI T. Relationship among Tresca, Mises, Mohr-Coulomb and Matsuoka-Nakai failure criterion [J]. Soils and Foundations, 1985, 25(4): 123−128.

[16] LADE P V. Modeling failure in cross-anisotropic frictional materials [J]. International Journal of Solids and Structures, 2007, 44: 5146−5162.

[17] NG T T. Behavior of gravity deposited granular material under different stress paths [J]. Canadian Geotechnical Journal, 2005, 42: 1644−1655.

[18] KARSTUNEN M, KRENN H, WHEELER S J, KOSKINEN M, ZENTAR R. Effect of anisotropy and destructuration on the behavior of Murro test embankment [J]. International Journal of Geomechanics, 2005, 5(2): 87−97.

[19] SOROUSH A, ARAEI A A. Analysis of behaviour of a high rockfill dam [J]. Geotechnical Engineering, 2006, 159: 49−59.

[20] VARADARAJAN A, SHARMA K G, VENKATACHALAM K, GUPTA A K. Testing and modeling two rockfill materials [J]. Journal of Geotechnical and Geoenvironmental Engineering, 2003, 129(3): 206−218.

[21] DIHORU L, MUIR WOOD D, SADEK T, LINGS M. A neural network for error prediction in a true triaxial apparatus with flexible boundaries [J]. Computers and Geotechnics, 2005, 32: 59−71.

[22] DUNCAN J M, BYRNE P M, WONG K S. Strength，stress-strain and bulk modulus parameters for finite element-analysis of stress and movements in soil masses (VCB/GT/78 — 02) [R]. Berkeley: University of California, 1978.

[23] ZIENKIEWICZ O C, PANDE G N. Some useful forms of isotropic yield surfaces for soil and rock mechanics [C]// Finite Elements in Geomechanics. New York: John Wiley & Sons, 1977: 179−190.

[24] SHI Wei-cheng, ZHU Jun-gao, LIU Han-long. Influence of intermediate principal stress on deformation and strength of gravel [J]. Chinese Journal of Geotechnical Engineering, 2008, 30(10): 1449−1453. (in Chinese)

(Edited by CHEN Wei-ping)